American Mineralogist, Volume 92, pages 753–760, 2007

Optical absorption study of natural garnets of almandine-skiagite composition showing intervalence $Fe^{2+} + Fe^{3+} \rightarrow Fe^{3+} + Fe^{2+}$ charge-transfer transition

MICHAIL N. TARAN,[1,*] M. DARBY DYAR,[2] AND STANISLAV S. MATSYUK[1]

[1]Institute of Geochemistry, Mineralogy and Ore Formation, National Academy of Sciences of Ukraine, Palladin Avenue 34, Kiev-142, 252680 Ukraine
[2]Mount Holyoke College, 50 College Street, South Hadley, Massachusetts 01075, U.S.A.

ABSTRACT

A broad (FWHM ≈ 7300 cm^{-1}) intense band at ~21 700 cm^{-1} in the optical absorption spectra of natural Fe^{2+}, Fe^{3+}-rich garnets is attributed to electronic intervalence charge-transfer transitions (IVCT), $^{VIII}Fe^{2+} + {}^{VI}Fe^{3+} \rightarrow {}^{VIII}Fe^{3+} + {}^{VI}Fe^{2+}$. In Fe^{3+}, Fe^{2+}-bearing garnets of predominantly almandine compositions, this band causes yellowish tinges in addition to the pink color, typical of pure Fe^{3+}-free almandines. In garnets from deeper-seated mafic granulites from kimberlite pipes in Siberia with high skiagite ($Fe_3^{2+}Fe_2^{3+}Si_3O_{12}$) contents, IVCT causes intense brownish-yellow colors. The relatively high energy of the band (~21 700 cm^{-1}) compared to diverse minerals showing IVCT between Fe^{2+} and Fe^{3+} in adjacent octahedral sites, is attributed to the charge-transfer transition taking place between Fe^{2+} and Fe^{3+} in non-equivalent, dodecahedral and octahedral sites of the garnet structure. Band intensity is directly correlated with the product of Fe^{2+} and Fe^{3+} as measured by Mössbauer spectroscopy. The energy of the IVCT band is nearly independent of temperature, whereas its intensity decreases slightly with increasing temperature. Pressure induces a weak shift of the band to lower energies, $\Delta\nu/\Delta P \approx -75$ cm^{-1}/GPa, but intensity of the bands remains practically unchanged. Such temperature and pressure dependencies are quite different from those in other minerals showing IVCT between Fe^{2+} and Fe^{3+} in equivalent octahedral positions of structure.

Keywords: Garnets, optical absorption spectra, Mössbauer spectra, iron ions, electronic dd transitions, intervalence charge-transfer transitions

INTRODUCTION

Intervalence charge transfer (IVCT) optical absorption bands ($Fe^{2+} + Fe^{3+} \rightarrow Fe^{3+} + Fe^{2+}$ and $Fe^{2+} + Ti^{4+} \rightarrow Fe^{3+} + Ti^{3+}$) commonly observed in the optical spectra of many oxygen-based minerals (Burns 1993), seldom occur in garnet. The literature contains only a few publications devoted to optically induced IVCT processes in garnets, mostly those with relatively high Fe and Ti-contents. Moore and White (1971) observed a broad band in the near-infrared region at ~5280 cm^{-1} in spectra of Ti-enriched melanites. It was attributed to $Fe^{2+} + Ti^{4+} \rightarrow Fe^{3+} + Ti^{3+}$ IVCT electronic transitions, assuming that Fe^{2+} and Ti^{4+} ions enter dodecahedral and tetrahedral positions, respectively, of the garnet structure. Later, Taran et al. (1978) and then Platonov et al. (1991) attributed a broad intense band at ~23 500 cm^{-1} in spectra of Fe and Ti-bearing natural garnets from mantle eclogites to represent $Fe^{2+} + Ti^{4+} \rightarrow Fe^{3+} + Ti^{3+}$ IVCT between Fe^{2+} and Ti ions in, respectively, dodecahedral and octahedral sites of the structure. Last, IVCT between Fe^{2+} and Fe^{3+} in dodecahedral and octahedral sites was observed by Khomenko et al. (1993a, 1993b) in spectra of synthetic garnets of skiagite ($Fe_3^{2+}Fe_2^{3+}Si_3O_{12}$) to almandine ($Fe_3^{2+}Al_2^{3+}Si_3O_{12}$) composition as a broad intense band with maximum at about 20 500 cm^{-1}.

The relatively low probability for Fe^{2+}/Ti^{4+} and, especially, Fe^{2+}/Fe^{3+} IVCT transitions in garnets is most likely related to peculiarities of the garnet structure. In contrast to most minerals, wherein optically induced Fe^{2+}/Fe^{3+} IVCT processes are widespread (micas, clinopyroxenes, amphiboles etc.), the garnet structure does not contain equivalent edge- or face-sharing cation sites that can accommodate Fe^{2+}/Fe^{3+} intervalent pairs. In the silicate garnet structure, such Fe^{2+} and Fe^{3+} predominantly enter the edge-sharing dodecahedral and octahedral sites, respectively, which have relatively long intercationic distances [3.20–3.25 Å from pyrope to spessartine (Novak and Gibbs 1971)]. Therefore, the intervalent Fe^{2+}/Fe^{3+} ion pairs in the garnet structure are rare and of a rather asymmetrical character (cf. Sherman 1987). Garnet IVCT transitions, if they exist, should appear at higher energies than those arising from symmetrical Fe^{2+}/Fe^{3+} IVCT bands in other minerals. Therefore, delocalization of the *d*-electron along Fe^{2+}-Fe^{3+} bond and the resultant electronic Fe^{2+}/Fe^{3+} IVCT transitions in garnets may have relatively low probabilities. Perhaps for these reasons, in spite of relatively high contents of $^{VIII}Fe^{2+}$ and $^{VI}Fe^{3+}$ in many of them, natural garnets usually do not show any significant absorption in the spectral range from ca. 12 000 to 16 000 cm^{-1} where $Fe^{2+} + Fe^{3+} \rightarrow Fe^{3+} + Fe^{2+}$ IVCT transitions occur in other minerals (Burns 1993). Thus, $Fe^{2+} + Ti^{4+} \rightarrow Fe^{3+} + Ti^{3+}$ IVCT and, especially, $Fe^{2+} + Fe^{3+} \rightarrow Fe^{3+} + Fe^{2+}$ IVCT, the latter having much smaller oscillator strength than the former one (Mattson and Rossman 1987), should be observed only in garnets with high concentrations of relevant

* E-mail: taran@igmr.relc.com

0003-004X/07/0506–753$05.00/DOI: 10.2138/am.2007.2163

intervalent ions at energies noticeably higher than in minerals with octahedral Fe^{2+} and Ti^{4+}, or Fe^{2+} and Fe^{3+} in adjacent sites. In the latter case of Fe^{2+}/Fe^{3+} IVCT, these should be garnets of high almandine contents with relatively high concentrations of $^{VI}Fe^{3+}$. Appropriate brownish-yellow garnets with unusually high contents of the skiagite component ($Fe_3^{2+}Fe_2^{3+}Si_3O_{12}$) were found in mafic granulites of Eastern Siberia. Petrography and mineralogy of this locality were described in detail by Spetsius and Serenko (1990). It is assumed that these rocks had crystallized at depth in the upper mantle. Due to high concentrations of $^{VIII}Fe^{2+}$ and $^{VI}Fe^{3+}$, these garnets seem to be the most probable candidates for finding electronic $Fe^{2+} + Fe^{3+} \rightarrow Fe^{3+} + Fe^{2+}$ IVCT between Fe^{2+} and Fe^{3+} in adjacent eight- and sixfold positions of the garnet structure. To prove this suggestion, we studied the optical absorption spectra of such garnets at different temperatures and pressures. Four garnets of other (crustal) origins having relatively high $^{VIII}Fe^{2+}$ and $^{VI}Fe^{3+}$ content, were also studied for comparison. Microprobe analysis and Mössbauer spectroscopy were applied to evaluate the Fe^{2+} and Fe^{3+} contents in the garnets studied.

Sampling and experimental method

Localities, host rocks, and colors of the garnets are shown in Table 1. The garnets occur as relatively large (up to ca. 2 mm) crystals or aggregates. Transparent, homogeneously colored grains were selected under a binocular microscope and prepared for optical spectroscopic measurements as doubly polished platelets with parallel faces and thicknesses of ~0.1 to 0.6 mm, depending on the intensity of their color. Thickness was measured with a micrometer.

Chemical analyses of the garnets were obtained with a Cameca SX100 electron microprobe at GeoForschungsZentrum (Potsdam, Germany), using rhodonite (Mn), Fe_2O_3 (Fe), rutile (Ti), wollastonite (Ca, Si), chromite (Cr), olivine (Mg), and Al_2O_3 (Al) as standards. The uncertainty of oxide content determination does not exceed 0.01 wt%. Garnet compositions averaged over 5 to 10 microprobe analyses, along with the formula proportions of cations based on 12 O atoms are compiled in Table 2. The formulae were calculated assuming the usual distribution of major elements Mg, Mn, Ca in the dodecahedral, and Al in the octahedral sites, respectively, of the garnet structure; a part of the Al was sited in tetrahedra to compensate for the deficiency of Si. To confirm the lack of ^{IV}Fe in the garnets, single-crystal X-ray structures were determined for three samples, UEP-1/77, GTF 90-33, and YuK-371/77, using a Bruker diffractometer equipped with a 4K Apex CCD detector at Miami University (Oxford, OH). In the final refinements, the scattering of the tetrahedral site was allowed to vary without constraints. In all cases, the electron occupancy of the site diminished slightly from that of a site completely occupied by Si, confirming the lack of any heavy scatterer (e.g., Fe) at the tetrahedral site (J.M. Hughes, personal communication, 2006).

Iron was allocated into both the dodecahedral and the octahedral sites as Fe^{2+} and Fe^{3+}, respectively, whereas minor amounts of Cr and Ti were sited into the octahedral positions. This procedure results in considerable amounts of both Fe^{2+} in dodecahedral sites (ranging from ca. 1.1 to 1.8 apfu), and Fe^{3+} in octahedral ones (from 0.05 to 0.12 apfu) in all samples studied.

Optical absorption spectra were measured in the range 330–1800 nm (ca. 30 000–5555 cm^{-1}) with a single-beam microspectrophotometer constructed on the basis of a SpectraPro-275 triple grating monochromator, highly modified polarizing mineralogical microscope MIN-8, and an IBM PC at the Institute of Geochemistry, Mineralogy and Ore Formation (Kiev, Ukraine). Ultrafluars 10× lenses served as the objective and condenser. Changeable photomultiplier tubes and a cooled PbS-cell were used as photodetectors. A mechanical-high-stability 300 Hz-chopper and lock-in amplifier were applied to improve the signal/noise ratio. The spectra were scanned with steps $\Delta\lambda$ = 1 nm and 2 nm in the range 330–1000 and 1000–1800 nm, respectively. The spectral slit width did not exceed 1 nm in the whole range studied. The diameter of the measured spot was not larger than 400 μm. All spectra are normalized to 1.0 cm thickness. The resultant linear absorption coefficient was then plotted versus the wavenumber.

Optical absorption spectra at liquid nitrogen temperature (~77 K) were measured using a home-made miniature cryostat attached to the microspectrometer. The samples were placed on a transparent supporting plate prepared from synthetic high-quality single-crystal sapphire. Because the thermal conductivity of Al_2O_3 at low temperature is almost twice that of annealed pure copper (Volkov et al. 1981), it provides a good thermal conductivity between the samples and sample holder of the cryostat. To maintain thermal contact, the sample was attached first to the supporting plate then to the cooled sample holder with an organic glue. The cryostat was evacuated to a pressure of ~10^{-3} torr. To avoid moisture condensation, the external surfaces of the windows were continuously blown with dry air.

For high-temperature spectral measurements (up to 400 °C), a sample was sited into a small furnace mounted on the microscope stage. A special homemade electronic device allowed stabilization of the temperature of the sample to within ±1 °C. A running water outer circle prevented heating of the microscope stage during the measurements.

Diamond anvil cell techniques were used to obtain the high-pressure electronic absorption spectra (up to ca. 10 GPa) and are described elsewhere (e.g., Langer 1990). The gasket was machined from hardened steel, 300 μm thick with a 300 μm diameter bore. A 4:1 mixture of methanol:ethanol served as the pressure-transmitting medium. The ruby fluorescence method was used for pressure calibration (Mao et al. 1979). The estimated precision of the pressure determination is ±0.18 GPa (Langer et al. 1997).

Optical absorption spectra were fitted with Gaussian components using Jandel Scientific software Peakfit 4.11. The main limitation of the procedure is the choice of a lineshape for the strong high-energy absorption edge overlapping the UV and part of the visible range in most of our spectra. This uncertainty frequently results in appreciable differences in energies, intensities, and widths of component Gaussian bands in spectra of different samples. On the basis of our experience with the set of spectroscopic functions available in Peakfit 4.11, the absorption edge is usually fit best by a sum of Gaussian and Lorentzian curves.

For Mössbauer analysis, approximately 2–30 mg of each sample were crushed to a fine powder with sugar under acetone before mounting in a sample holder confined by cellophane tape. Mössbauer spectra were acquired at Mount Holyoke College at 295 K using a source of 100–90 mCi ^{57}Co in Rh on a WEB Research Co. model WT302 spectrometer. Run times were 6–24 h, and results were calibrated against α-Fe foil; baseline counts were ~14 million for sample YuK-371/77 and 2–5 million for all others. Spectra were processed using the DIST_3D program, an implementation of software described in Wivel and Mørup (1981). The program uses quadrupole splitting distributions with Lorentzian lineshapes and an assumed average correlation between the isomer shift and quadrupole shift in each of two valence states. Widths, isomer shifts (IS), and quadrupole splittings (QS) of the doublets were allowed to vary. Errors on the isomer shift and quadrupole splitting of well-resolved peaks were usually ±0.02 mm/s, and errors on peak areas were probably ±1–2% absolute on these well-resolved spectra.

To determine the number of Fe^{3+} and Fe^{2+} cations per formula unit, the final Mössbauer peak areas were corrected to account for differential recoil-free fractions (f) of Fe^{3+} and Fe^{2+}. For this calculation, we used a value of C = 1.27 based on the work of Whipple (1973), in which Fe^{3+}/Fe^{2+} derived from Mössbauer spectra of garnets were compared with wet-chemical results. The formulation is:

$$\frac{A^{Fe^{3+}}}{A^{Fe^{2+}}} = C\frac{N^{Fe^{3+}}}{N^{Fe^{2+}}}$$

where A is the doublet area of Fe^{2+} or Fe^{3+}, and N is the "true" amount of that species

Table 1. Colors, localities, and occurrences of the garnets studied

Sample no.	Color	Locality	Occurrence
SM 1348	yellowish-pink	Gore Mountain, Essex Co. NY	porphyroblast in gabbro
GTF 90-33	orange-pink	De Luca pit, Emery Hill, Cortlandt, NY	hornfels
GTF 90-28	pink	Fort Wrangle, Alaska	schist
WGR 1R	yellowish-pink	West Garnet Ridge, Arizona	xenocryst in ultra mafic dike
2152	brownish-yellow	Udachnaya kimberlite pipe, Siberia	xenolith of mafic granulite
UEP-1/77	brownish-yellow	Udachnaya kimberlite pipe, Siberia	xenolith of mafic granulite
YuK-371/77	dark brownish-yellow	Jubileinaya kimberlite pipe, Siberia	xenolith of mafic granulite

Table 2. Microprobe compositions along with the resultant numbers of cations based on 12 O atoms and crystal chemical formulae of the garnets studied

Element	GTF 90-28	SM 1348	WGR 1R	GTF 90-33	UEP-1/77	2152	YuK-371/77
wt% SiO_2	37.93	39.31	39.70	39.34	38.40	38.12	36.75
wt% TiO_2	0.02	0.05	0.03	0.16	0.09	0.12	0.22
wt% Al_2O_3	21.34	22.11	22.21	21.97	21.35	20.89	20.43
wt% Cr_2O_3	0.04	0.02	0.04	0.03	0.00	0.02	0.13
wt% FeO*	32.99	21.40	21.17	23.42	27.44	26.92	28.82
wt% MnO	0.81	0.43	0.71	0.95	0.56	0.60	1.23
wt% MgO	5.78	11.38	9.90	11.82	7.00	6.49	4.93
wt% CaO	1.67	5.10	6.89	2.46	5.46	6.66	5.71
Total	100.57	99.79	100.65	100.16	100.30	99.82	98.20
MS %Fe^{3+}†	0	3	3	4	6	6	12
wt% FeO†	32.99	20.76	22.72	20.32	25.30	25.79	25.36
wt% Fe_2O_3†	0.00	0.71	0.78	1.80	1.80	1.83	3.84
^{IV}Si	2.961	2.971	2.952	2.990	2.980	2.964	2.937
^{IV}Al	0.039	0.029	0.048	0.010	0.020	0.036	0.063
^{VI}Al	1.995	1.941	1.899	1.958	1.933	1.879	1.861
^{VI}Cr	0.001	0.001	0.002	0.002	0.000	0.001	0.008
$^{VI}Fe^{3+}_{MS}$	0.000	0.040	0.044	0.103	0.105	0.107	0.231
^{VI}Ti	0.003	0.003	0.002	0.009	0.005	0.007	0.013
Sum VI	1.999	1.985	1.946	2.072	2.043	1.994	2.144
^{VIII}Mg	0.673	1.282	1.098	1.339	0.810	0.752	0.587
$^{VIII}Fe^{2+}$	2.153	1.312	1.413	1.291	1.642	1.677	1.695
^{VIII}Mn	0.054	0.028	0.045	0.061	0.037	0.040	0.083
^{VIII}Ca	0.140	0.413	0.549	0.200	0.454	0.555	0.489
Sum VIII	3.019	3.035	3.104	2.892	2.942	3.024	2.854

* All iron is determined on the EMPA as FeO. Fe^{2+} and Fe^{3+} were recalculated from the EMPA data by assuming the usual distribution of major elements Mg, Mn, and Ca in the dodecahedral and Al in the octahedral sites, respectively, of the garnet structure; a part of the Al was sited in tetrahedra to compensate for the deficiency of Si.
† Mössbauer data corrected for differential recoil-free fraction were combined with EMPA data to calculate the garnet formulas based on 12 O atoms.

present. Whipple's value, which is the largest obtained for any known silicate, is consistent with the value for *f* of Fe^{2+} in garnet obtained by Eeckhout and De Grave (2003) (unfortunately, there is no modern determination of *f* for Fe^{3+} in garnet).

Results

The absorption spectra of the studied garnets may be divided into two groups according to peak shape and intensity in the visible and near-UV ranges (Figs. 1a and 1b). Group I (Fig. 1a) consists of five garnets of presumably crustal origin displaying pink to orange-pink colors of different tinges. Group II consists of three brownish-yellow samples from the deeper-seated mafic granulites (cf. Table 1). The features common to most spectra are a strong UV absorption edge (Fig. 1) with a low-energy tail that reaches into the visible range, and two broad absorption bands *a* and *b* in the near IR (~7700 and ~5900 cm^{-1}). In addition, all garnets of the group I display a series of weak but prominent bands (labeled *c* to *j*). In spectra of Group II garnets, only the two last bands, *h* and *j*, are distinct, whereas all the others are probably overlapped by a broad intense band with a maximum at ~21 700 cm^{-1}, designated as IVCT (Fig. 1b). This band is obviously present in the spectra of some samples of group I (viz. the SM 1348, WGR 1R and, especially, GTF 90-33), though it is partly superimposed by the narrower and weaker bands *c* to *j* (Fig. 1a). The curve-fitting analyses, based on an assumption of Gaussian shape of the component bands and the absorption edge as a combination of Gaussian and Loretzian (Fig. 2), reveal that the IVCT band has a maximum at nearly 21 700 cm^{-1} and a half-width, i.e., the full width on half magnitude (FWHM), of about 7300 cm^{-1}. Note that several weaker components are necessary for a satisfactory fit. Most of them (*e*, *g*, *h,* and *j*), are the bands seen in the original spectra of, especially, the group I garnets (cf. Fig. 1a). A relatively strong and broad (FWHM ≈ 1100 cm^{-1}) *i*-band at around 26 500 cm^{-1}, marked by the filled

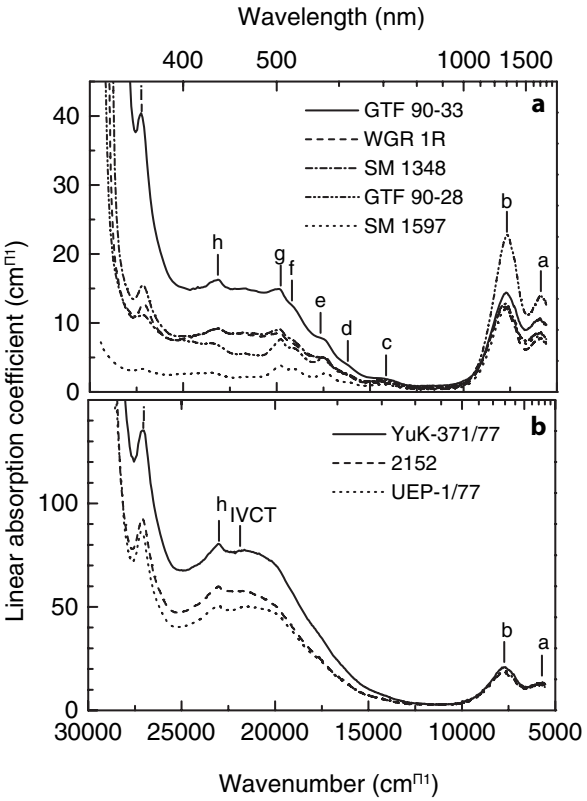

Figure 1. Optical-absorption spectra of natural garnet samples. (**a**) garnets of crustal origin of predominantly almandine composition; (**b**) garnets from mafic granulites with high skiagitic contents (Table 2) showing strong IVCT band.

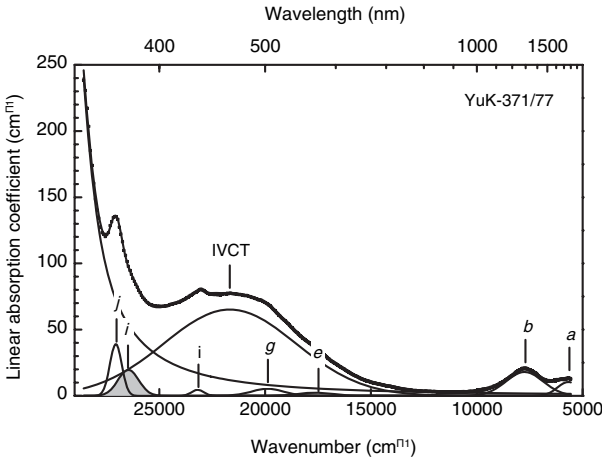

FIGURE 2. The result of the curve-fitting analysis of optical-absorption spectrum of garnet sample YuK-371/77 in the range 29 000–5000 cm^{-1}. All component bands are assumed to have Gaussian shape, whereas the absorption edge is simulated by a combination of Gaussian and Loretzian. Note that all component bands except the *i*-band (marked by the filled area) are seen in the original spectrum.

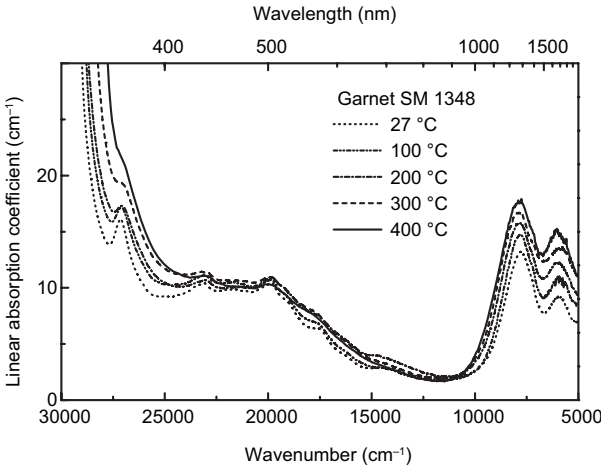

FIGURE 3. Optical-absorption spectra of garnet sample SM 1348 measured at different temperatures.

TABLE 3. Optical absorption bands in spectra of the garnets studied

Band	Energy, cm^{-1}	Ion	Electronic transition
a	5880	$^{VIII}Fe^{2+}$	$^5E_g \rightarrow {}^5T_{2g}$ *
b	7650	$^{VIII}Fe^{2+}$	$^5E_g \rightarrow {}^5T_{2g}$ *
c	14 370	$^{VIII}Fe^{2+}$	
d	16 200	$^{VIII}Fe^{2+}$	$^5E_g \rightarrow {}^3T_{1g}$ (^3H) †
e	17 410	$^{VIII}Fe^{2+}$	
f	19 100	$^{VIII}Fe^{2+}$	$^5E_g \rightarrow {}^3E_{1g}$ (^3H) †
g	19 780	$^{VIII}Fe^{2+}$	
IVCT	21 700	$^{VIII}Fe^{2+}$, $^{VI}Fe^{3+}$	$^{VIII}Fe^{2+} + {}^{VI}Fe^{3+} \rightarrow {}^{VIII}Fe^{3+} + {}^{VI}Fe^{2+}$ ‡
h	23 000	$^{VI}Fe^{3+}$	$^6A_{1g} \rightarrow {}^4A_{1g}$, ^4E_g (^4G) †
i	26 420	$^{VI}Fe^{3+}$	$^6A_{1g} \rightarrow {}^4T_{2g}$ (^4D) ‡
j	27 100	$^{VI}Fe^{3+}$	$^6A_{1g} \rightarrow {}^4E_g$ (^4D) †

*White and Moore (1972).
† Moore and White (1972).
‡ This work.

area in Figure 2, is necessary for fitting, although this band is not individually resolved in the original spectra. All bands observed in spectra of the garnets studied here, along with their attribution to electronic transitions in Fe ions, are listed in Table 3.

Upon heating, as seen in Figure 3 for the group I garnet SM 1348, the intensity of UV absorption edge strongly increases. The two NIR bands, *a* and *b*, become broader and display a distinct intensification at increasing temperature. Energies of these bands slightly increase, changing from ~5900 and 7700 cm^{-1} at room temperature, 27 °C, to ~6100 and ~7900 cm^{-1} at 400 °C. The narrow *c* to *j* bands become broader and weaker and, thus, less distinct against the growing absorption edge. The IVCT band, as seen from the spectra, does not display any significant variations with temperature. Taking into consideration strong intensification of the absorption edge, it appears that its intensity somewhat decreases with heating. This is also seen from the spectra of the group II garnet YuK-371/77, measured at different temperatures (Fig. 4): the intensity of the IVCT band changes slightly when an increase of the background is taken into consideration. The curve-fit analysis shows that during heating from room temperature to 400 °C, linear intensity of the band slightly decreases from ca. 65 to 60 cm^{-1}, respectively, whereas its width does not change much.

As temperatures decrease from ca. 297 to 80 K (not shown), the above-mentioned trends hold: at decreasing temperature, the edge shifts to higher energies, while all bands become narrower and thus better resolved. This is especially true for sharp bands like *g*, *h,* or, in particular, *j*, although the energies of such bands change only slightly. The two most prominent and narrow bands *h* and *j*, for instance, shift from 23 090 to 22 920 cm^{-1} and from 27 350 to 27 080 cm^{-1} over the temperature range from 77 K (–296 °C) to 573 K (300 °C). With cooling to 77 K, the IVCT band becomes better resolved, although its intensity does not significantly change.

Pressure appreciably affects the spectra. This is shown in Figure 5 for the group II garnet YuK-371/77, which has the most intense IVCT band of all the garnets studied (cf. Fig. 1). As pressure increases from ambient conditions to 9.31 GPa, the absorption edge shifts to higher energies and the two narrow bands *h* and *j* grow in intensity, such that the latter one shifts slightly to lower energy (ca. 27 120 and 27 040 cm^{-1}), whereas the former band remains practically unchanged. The IVCT band shifts to lower energy without any noticeable change in intensity. The energy of the IVCT band is estimated to decrease from ca. 21 650 to 20 950 cm^{-1} over the range of $\Delta\nu/\Delta P \approx -75$ cm^{-1}/GPa.

Four representative Mössbauer spectra of the garnets studied are shown in Figure 6, and corresponding Mössbauer parameters are presented in Table 4. In all spectra, the predominant absorption feature is an intense quadruple doublet at ~–0.48 and 3.07 mm/s, corresponding to $^{VIII}Fe^{2+}$. In all but two spectra, two components representing $^{VIII}Fe^{2+}$ were needed to obtain good fits. These Fe^{2+} doublets have isomer shifts (IS) of ~1.29 and 1.32–1.43 mm/s and quadrupole splittings (QS) of ~3.57 and 3.29–3.53 mm/s, respectively. These doublets represent two different populations (here designated $^{VIII}Fe_1^{2+}$ and $^{VIII}Fe_2^{2+}$) of nearest and next-nearest neighbors around the $^{VIII}Fe^{2+}$ (as observed in, for example, pyroxenes). As seen from Table 4, two garnets, SM 1348 and WGR 1R, need the largest contribution of $^{VIII}Fe_2^{2+}$, with areas similar to $^{VIII}Fe_1^{2+}$. It is noteworthy that the microprobe compositions (Table 2) of these two samples have the lowest $^{VIII}Fe^{2+}$ contents among all garnets studied; i.e., their

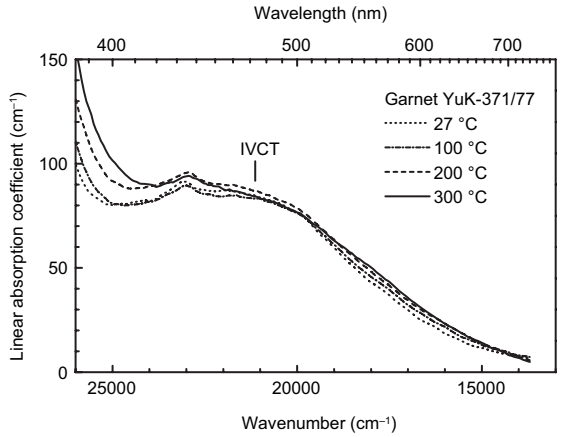

FIGURE 4. Optical-absorption spectra of garnet sample YuK-371/77 measured at different temperatures.

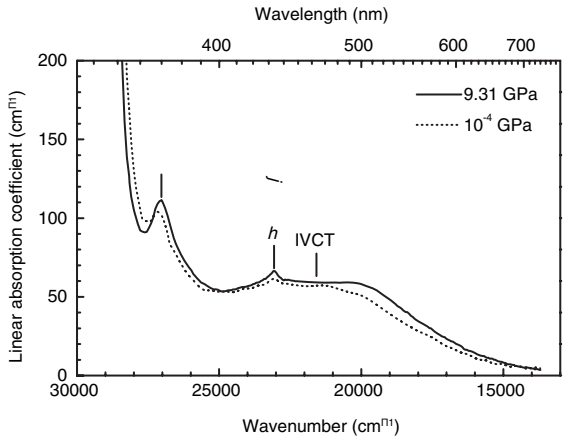

FIGURE 5. Optical-absorption spectra of garnet sample YuK-371/77 measured at two different pressures.

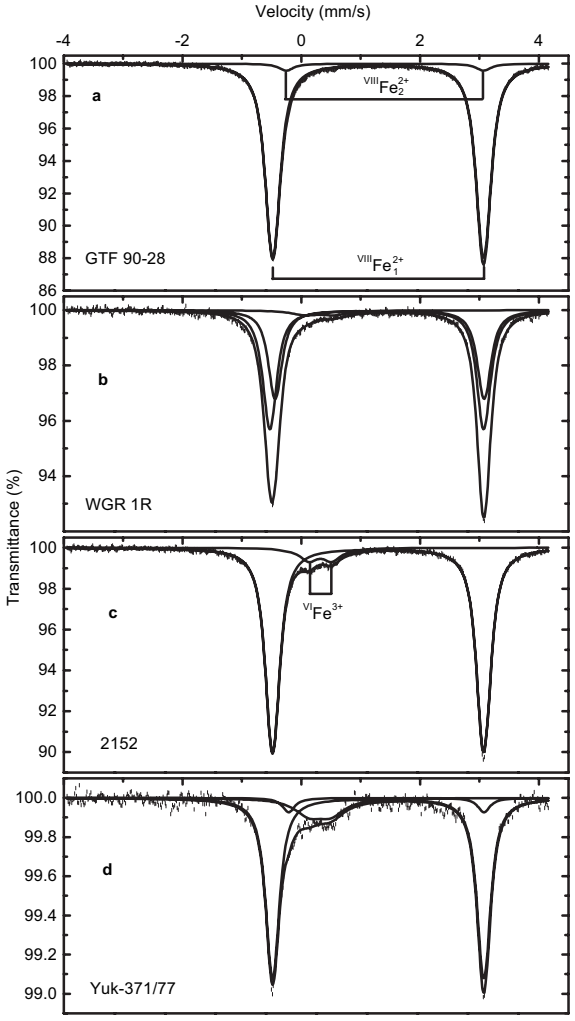

FIGURE 6. Representative Mössbauer spectra of the garnets samples studied here. Two quadrupole doublets representing contributions from $^{VIII}Fe^{2+}$ were used in our fits, representing the almandine component. A smaller doublet assigned to $^{VI}Fe^{3+}$ represents the andradite component.

compositions deviate to a larger extent from pure almandine than do the other samples. Perhaps the additional Mg in the structure is creating the two different environments represented by the two Fe^{2+} subcomponents.

Finally, we note that all garnets except sample GTF 90-28 also contain a small amount of $^{VI}Fe^{3+}$. Parameters for this doublet are IS = 0.31 mm/s and QS = 0.34–0.50 mm/s, analogous to those observed by Dyar (1984) for Fe^{3+} in andradite.

DISCUSSION

Based on the chemical compositions and crystal-chemical formulae of the garnets studied (Table 2), two species should be expected in their optical-absorption spectra: specifically, *dd* electronic transitions caused by Fe^{2+} and Fe^{3+}, both very well studied by now. Indeed, in spectra of natural garnets, especially those of the pyrope-almandine-spessartine group, $^{VIII}Fe^{2+}$ ions usually produce three broad intense bands in the near-IR range around 7700, 5900, and 4500 cm^{-1}, caused by split spin-allowed *dd* transitions $^5E_g \rightarrow {}^5T_{2g}$, and a set of much weaker and narrower bands of spin forbidden transitions in the visible (e.g., Moore and White 1972; Burns 1993). Two of the three spin-allowed bands of $^{VIII}Fe^{2+}$, *a* and *b*, are seen in spectra of all garnets studied here (see Fig. 1) whereas the third one, at ~4500 cm^{-1}, is beyond the spectral range investigated. Intensities of the *a* and *b* bands vary in accordance with the $^{VIII}Fe^{2+}$ contents, reaching a maximum in the spectrum of GTF 90-28 (Fig. 1a), which has the largest Fe^{2+} content of all the garnets studied (Table 2). A series of weak bands from *c* to *g* arises from the spin-forbidden transitions of $^{VIII}Fe^{2+}$ (Table 3). Their shape and energies are practically identical to those described elsewhere (e.g., Manning 1967a, Moore and White 1972). The temperature-induced intensifications of the *a* and *b* bands (Fig. 3) and their weak shifts to higher energies confirm the observations of White and Moore (1972) and Taran and Langer (2001).

A pair of bands, designated as *h* and *j*, are evidently related to the absorption edge. These bands are weak in the spectrum of GTF 90-28 (Fig. 1a), where the edge is weakest, but reach

TABLE 4. Mössbauer parameters

Sample	$^{VIII}Fe_1^{2+}$				$^{VIII}Fe_2^{2+}$				$^{VI}Fe^{3+}$					
	IS	QS	Γ	Area	IS	QS	Γ	Area	IS	QS	Γ	Area	χ^2	%Fe^{3+}
GTF 90-28	1.29	3.55	0.26	96	1.41	3.33	0.28	4					2.00	0
SM 1348	1.28	3.59	0.24	54	1.32	3.53	0.24	42	0.31	0.40	0.56	4	1.15	3
WGR 1R	1.27	3.59	0.24	55	1.32	3.52	0.24	41	0.31	0.50	0.55	4	0.88	3
GTF 90-33	1.29	3.57	0.24	85	1.37	3.42	0.24	10	0.31	0.34	0.59	5	0.75	4
UEP-1/77	1.30	3.56	0.27	93					0.31	0.38	0.43	7	3.98	6
2152	1.29	3.56	0.25	92					0.32	0.38	0.35	8	1.46	6
YuK-371/77	1.30	3.56	0.24	80	1.43	3.29	0.24	6	0.31	0.37	0.57	14	0.77	12

Notes: IS is isomer shift, QS is quadruple splitting, Γ is half-width of the doublet peaks, χ^2 reflects the goodness of the fit, and %Fe^{3+} is calculated by using a correction factor (C = 1.27) to relate the peak areas to the abundance of Fe^{3+} and Fe^{2+}; see text and Whipple (1973) for explanation.

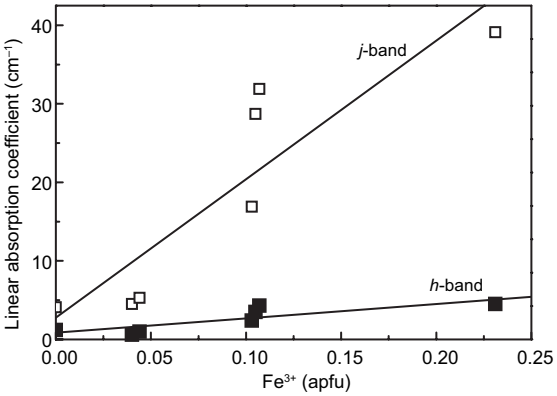

FIGURE 7. Plot of linear intensity of the *j*- and *h*-bands in optical-absorption spectra of the garnets studied vs. $^{VI}Fe^{3+}_{MS}$ apfu (taken from Table 2).

their maxima in the spectra of the group II garnets, all of which have a very strong edge (Fig. 1b). Taking into consideration the energies and shapes of these two bands, the compositions of the garnets studied, their Fe^{3+} contents, (Table 2), as well as the numerous published data (e.g., Manning 1967b; Taran et al. 1978; Burns 1993), these bands can confidently be assigned to the electronic spin-forbidden transitions $^6A_{1g} \rightarrow {}^4A_{1g}, {}^4E_g$ (^4F) and $^6A_{1g} \rightarrow {}^4E_g$ (^4D), respectively, of Fe^{3+} in octahedral sites of the garnet structure (Table 3). The absorption edge is undoubtedly due to the Fe^{3+} content, being most probably caused by ligand-to-metal charge-transfer transitions of $O^{2-} \rightarrow Fe^{3+}$ type. Figure 7 shows the dependencies of the linear intensity of the *h*- and *j*-band, derived by the curve resolution (see Fig. 2), on molar $^{VI}Fe^{3+}$ content (Table 2). As seen, they can be approximated well by linear functions, again in agreement with the assumption that the bands are caused by $^{VI}Fe^{3+}$.

In the spectra of andradites (demantoids) and Fe^{3+}-bearing grossularites, $^{VI}Fe^{3+}$ usually causes three weak spin-forbidden bands typical of $3d^5$-electronic configurations: $^6A_{1g} \rightarrow {}^4T_{1g}$, $^6A_{1g} \rightarrow {}^4T_{2g}$ and $^6A_{1g} \rightarrow {}^4A_{1g}, {}^4E_g$ (e.g., Manning 1967b; Taran et al. 1978). The latter band, much narrower and more intense then the two others, frequently occurs in spectra of many Fe^{3+}-bearing garnets at about 23 000 cm^{-1}, sometimes in combination with bands of other transition-metal ions. As stated above, this band of $^{VI}Fe^{3+}$, the *h*-band, is seen at nearly the same energy in the spectra of our garnets (Fig. 1), whereas the two other bands at lower energies, $^6A_{1g} \rightarrow {}^4T_{1g}$ and $^6A_{1g} \rightarrow {}^4T_{2g}$, do not appear. Note that the energies of bands *h* and *j*, 23 000 and 27 000 cm^{-1}, respectively, in our spectra of natural garnets are close to those observed in synthetic skiagite-almandine garnets, viz. 22 830 and 26 800 cm^{-1}, also interpreted as $^6A_{1g} \rightarrow {}^4A_{1g}, {}^4E_g$ and $^6A_{1g} \rightarrow {}^4E_g$ (^4D) transitions of $^{VI}Fe^{3+}$ (Khomenko et al. 1993a). A relatively broad *i*-band at around 26 420 cm^{-1} that results from the curve fitting procedure (the filled band in Fig. 2), may in this case be attributed to the $^6A_{1g} \rightarrow {}^4T_{2g}$ (^4D) transition of $^{VI}Fe^{3+}$. Note that its peak intensity versus $^{VI}Fe^{3+}_{MS}$-content (Table 2) can be closely approximated by a linear function ($r \approx 0.95$), which is consistent with our interpretation.

Weak temperature and, especially, pressure dependence of the energies of the *h*- and *j*-bands is also consistent with their assignment to the $^6A_{1g} \rightarrow {}^4A_{1g}$, ^4E_g and $^6A_{1g} \rightarrow {}^4E_g$ transitions of Fe^{3+}. Indeed, according to crystal-field theory, both transitions of the $3d^5$-configuration are independent of crystal-field strength, being functions of the Racah parameters *B* and *C* only (e.g., Burns 1993). As a result, their energies weakly depend on interatomic distances (e.g., Taran and Langer 2000), which vary appreciably under thermal expansion or hydrostatic compression. Therefore, the weak temperature- or pressure-induced shifts of the bands in question reflect mostly a change in the character of the chemical bond in the $Fe^{3+}O_6$-octahedra. Note also that the weak, almost negligible, pressure-induced shifts of the bands to lower energies are in agreement with observations of Khomenko et al. (1993a) on a synthetic skiagite-almandine garnet.

On the other hand, dependence of the intensities of the *h* and *j*-bands, as well as their absorption edges, on pressure in natural and synthetic samples is rather different. In synthetic samples, the intensity of the *j*-band decreases and that of the *h*-band changes hardly at all (Khomenko et al. 1993a); in the natural garnet YuK-371/77, intensities of both bands, especially the *j*-band, significantly increase (Fig. 5). Similarly, in synthetic skiagite-almandine garnet, the absorption edge and the IVCT bands "do not intensify significantly at the elevated pressure up to 120 kbar" (Khomenko et al. 1993a), whereas in our natural sample, the edge evidently shifts to higher energies (Fig. 5). The reason for pressure-induced intensification of the spin-forbidden *dd*-bands is not quite clear, especially when the "blue" shift of the UV absorption edge is taken into account, i.e., of the UV $O^{2-} \rightarrow Fe^{3+}$ charge-transfer transition from which spin-forbidden transitions may "borrow" their intensities (Ballhausen 1979).

It is reasonable to assume that the broad intense band labeled as IVCT (Figs. 1–3, 5), which appears in the spectra of Fe^{2+}- and Fe^{3+}-bearing garnets in addition to the crystal-field bands of $^{VIII}Fe^{2+}$ and $^{VI}Fe^{3+}$, is caused by an interaction of these two ions. Indeed, as follows from the compositions (Table 2), the garnets contain no other transition metals of significant amounts that could be responsible for this band, except, perhaps, $^{VIII}Mn^{2+}$.

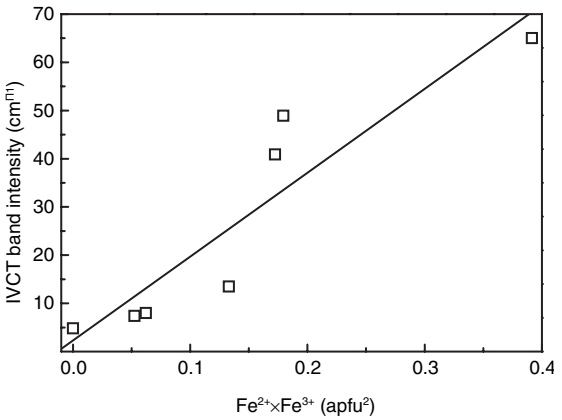

FIGURE 8. Plot of linear intensity of the IVCT band in optical-absorption spectra of the garnets studied vs. the product of $^{VIII}Fe^{2+}$ and $^{VI}Fe^{3+}_{MS}$ apfu (taken from Table 2).

However, all electronic *dd*-transitions of this ion are spin-forbidden (electronic d^5-configuration). At sufficiently high concentrations of $^{VIII}Mn^{2+}$, spectra of predominantly spessartine garnets may contain relatively narrow bands that, however, significantly differ in shape, width, and energy from the band in question (e.g., Manning 1967a; Slack and Chrenko 1971; Moore and White 1972). Furthermore, the intensity of the IVCT band does not correlate with Mn-contents (cf. Fig. 1, Table 2). However, as seen in Figure 8, the intensity of the IVCT band does correlate in a linear fashion (with $r = 0.922$) with the product of $^{VIII}Fe^{2+}$- and $^{VI}Fe^{3+}$-concentrations. Note that the correlation with $^{VI}Fe^{3+}$- or, especially, $^{VIII}Fe^{2+}$-content is noticeably lower, $r = 0.89$ and 0.16, respectively. Thus, we believe that the band in question is caused by $^{VIII}Fe^{2+} + {}^{VI}Fe^{3+} \rightarrow {}^{VIII}Fe^{3+} + {}^{VI}Fe^{2+}$ IVCT. Moreover, a similar band appears in the spectrum of synthetic skiagite-almandine garnet, $Sci_{15}Alm_{85}$, which does not contain any other transition metals except Fe (Khomenko et al. 1993a, 1993b). [Khomenko et al. (1993a) evaluated the energy of the band in the synthetic almandine-skiagite as 20 500 cm^{-1}. However, the curve fitting of spectra of natural samples gives a somewhat higher energy, ~21 700 cm^{-1} (Fig. 2).] The large (when compare with spin-allowed *dd*-transition bands of $3d^N$-ions) half-width of the IVCT band, ~7300 cm^{-1}, agrees with this interpretation. Its relatively high energy, around 21 500 cm^{-1}, higher than in other minerals showing IVCT between Fe^{2+} and Fe^{3+} in adjacent octahedral sites (Burns 1993), may be due to the fact that in our case the charge-transfer process takes place between Fe^{2+} and Fe^{3+} ions in non-equivalent, dodecahedral and octahedral sites of the garnet structure. A similar situation is found in cordierite or tuhualite, where energies of the IVCT bands are also noticeably higher than usual due to the fact that the Fe^{2+}/Fe^{3+} IVCT process involves non-equivalent, octahedral and tetrahedral structural sites (e.g., Faye et al. 1968; Taran and Rossman 2001, respectively).

The energy of the IVCT band in the garnet spectra remains nearly constant at different temperatures, whereas its intensity displays a rather weak temperature dependence, showing (relative to the growing absorption edge) a moderate decrease with heating (Figs. 3 and 4). This again differs noticeably from the Fe^{2+}/Fe^{3+} IVCT bands in other minerals, where the ions occupy adjacent octahedral sites (Smith 1977; Smith and Strens 1976; Taran and Langer 1998). In such cases, the Fe^{2+}/Fe^{3+} IVCT bands intensities strongly decrease with temperature. Such temperature dependence results from the strongly asymmetric character of the IVCT transition in the garnet structure, which is caused by large differences between the electrical potentials of donor and acceptor ions in adjacent edge-sharing dodecahedral and octahedral positions (cf. Taran and Langer 1998). Probably, this also may be the reason for the pressure-induced shift of the band to lower energies (see Results) instead of the slight shift to higher energies that is usually displayed by more symmetric Fe^{2+}/Fe^{3+} IVCT bands (Taran and Langer 1998).

Note that in the spectrum of synthetic Fe-bearing ringwoodite, a high-pressure γ-phase of olivine $(Mg, Fe)_2SiO_4$, Keppler and Smyth (2005) observed an anomalously strong pressure-induced shift of the band at ~17 482 cm^{-1}, which they attributed to IVCT between Fe^{2+} and Fe^{3+} in the octahedral sites of the structure, to higher energies. In contrast, the pressure behavior of the IVCT band in the spectra of garnets is noticeably different from that of the spin-allowed *dd*-bands, which normally are shifted strongly to higher energies as a result of the shortening of interatomic distances in the coordination polyhedra under compression (e.g., Langer 1990; Burns 1993; Langer et al. 1997). Note that its $\Delta\nu/\Delta P$-value, –75 cm^{-1}/GPa (see the Results section), is close to that established on synthetic almandine-skiagite, –7 cm^{-1}/kbar (Khomenko et al. 1993a). This finding suggests that in spite of its large intensity and breadth, the band cannot be attributed to a spin-allowed *dd*-transition. Moreover, Fe^{2+} has no spin-allowed transitions in this range, whereas Fe^{3+} has no spin-allowed transitions at all (e.g., Burns 1993). As stated above, the most likely reason for the appearance of the band in question in absorption spectra of Fe^{2+}, Fe^{3+}-enriched natural garnets is some kind of interatomic interaction of Fe ions—most probably, $^{VIII}Fe^{2+} + {}^{VI}Fe^{3+} \rightarrow {}^{VIII}Fe^{3+} + {}^{VI}Fe^{2+}$ IVCT process.

ACKNOWLEDGMENTS

We thank Anne Hofmeister (Washington University in St. Louis, Missouri) for providing the samples of crustal origin and for a critical reading of the manuscript. Numerous comments and suggestions by Manfred Wildner (Vienna), the official reviewer, significantly helped to improve the manuscript. Also we are thankful to Z.V. Spetsius (Mirny, Russia) who kindly provided the sample 2152, John Hughes (Burlington, Vermont), John Rakovan, and Yun Luo (Oxford, Ohio) for reassuring XRD results.

REFERENCES CITED

Ballhausen, C.J. (1979) Molecular Electronic Structures of Transition Metal Complexes. McGraw-Hill, New York.

Burns, R.G. (1993) Mineralogical Application of Crystal Field Theory (2nd ed.), Cambridge University Press, U.K.

Dyar, M.D. (1984) Precision and interlaboratory reproducibility of measurements of the Mössbauer effect in minerals. American Mineralogist 69, 1127–1144.

——— (2006) Mars mineral spectroscopy data base. Garnet group minerals. http://www.mtholyoke.edu/courses/mdyar/database/index.shtml?group=garnet .

Eeckhout, S.G. and De Grave, E. (2003) Evaluation of ferrous and ferric Mössbauer fractions. Part II. Physics and Chemistry of Minerals, 30, 142–146.

Faye, G.H., Manning, P.G., and Nickel, E.H. (1968) The polarized optical absorption spectra of tourmaline, cordierite, chloritoid and vivianite: ferrous-ferric electronic interaction as a source of pleochroism. American Mineralogist, 53, 1174–1201.

Keppler, H. and Smyth, J.R. (2005) Optical and near infrared spectra of ringwoodite to 21.5 GPa: Implications for radiative heat transport in the mantle. American Mineralogist, 90, 1209–1212.

Khomenko, V.M., Andrut, M., Langer, K., and Woodland, A.B. (1993a). Optical absorption spectra of skiagite ($Fe^{2+}_3Fe^{3+}_2Si_3O_{12}$)-almandine ($Fe^{2+}_3Al^{3+}_2Si_3O_{12}$) garnet at high pressure and high temperature. Beih. z. Eur. Mineral. 5: 182

Khomenko, V.M., Langer, K., Woodland, A.B., Andrut, M., and Vishnevsky,

A.A. (1993b) Optical absorption spectra of synthetic skiagite ($Fe^{2+}_3Fe^{3+}_2Si_3O_{12}$) and natural Fe^{2+}, Fe^{3+}-bearing garnets. Terra abstracts, 5, 491.

Langer, K. (1990) High pressure spectroscopy. In: Mottana A, Burragato F (eds.) Absorption Spectroscopy in Mineralogy, 228–284, Elsevier.

Langer, K., Taran, M.N., and Platonov, A.N. (1997) Compression moduli of Cr^{3+}-centered octahedra in a variety of oxygen-based rock-forming minerals. Physics and Chemistry of Minerals, 24, 109–114.

Mao, H.K., Bell, P.M., Dunn, K.J., Chrenko, R.M., and De Vries, C. (1979) Absolute pressure measurements and analysis of diamonds subjected to maximum static pressures of 1.3±1.7 Mbar. Review of Scientific Instruments, 50, 1002–1009.

Manning, P.G. (1967a) The optical absorption spectra of the garnets almandine-pyrope, pyrope, and spessartite and some structural interpretations of mineralogical significance. Canadian Mineralogist, 9, 237–251.

——— (1967b) The optical absorption spectra of some andradites and the indication of the $^6A_{1g} \rightarrow {}^4A_{1g}, {}^4E_g(G)$transition in octahedrally bonded Fe^{3+}. Canadian Journal of Earth Sciences,4, 1039–1047.

Mattson, S.M. and Rossman, G.R. (1987) Identifying characteristics of charge transfer transitions in minerals. Physics and Chemistry of Minerals, 14, 94–99.

Moore, R.K. and White, W.B. (1971) Intervalence electron transfer effects in the spectra of melanite garnets. American Mineralogist, 56, 826–840.

——— (1972) Electronic spectra of transition metal ions in silicate garnets. Canadian Mineralogist, 11, 791–811

Novak, G.A. and Gibbs, G.V. (1971) The crystal chemistry of silicate garnets. American Mineralogist,56, 791–825.

Platonov, A.N., Langer, K., Matsuk, S.S., Taran, M.N., and Hu, X. (1991) $Fe^{2+} \rightarrow Ti^{4+}$ charge-transfer in garnets from mantle eclogites. European Journal of Mineralogy, 3, 19–26.

Sherman, D.M. (1987) Molecular orbital (SCF-X_α-SW) theory of metal-metal charge transfer processes in minerals. I. Applications to Fe^{2+}-Fe^{3+} charge transfer and "electron delocalization" in mixed-valence iron oxides and silicates. Physics and Chemistry of Minerals, 14, 355–363.

Spetsius, Z.V. and Serenko, V.P. (1990) Composition of continental upper mantle and lower crust beneath the Siberian platform. Nauka Publischers, Moscow (in Russian).

Slack, G.A. and Chrenko, R.M. (1971) Optical absorption of natural garnets from 1000 to 30000 wavenumbers. Journal of the Optical Society of America, 61, 1325–1329.

Smith, G. (1977) Low temperature optical studies of metal-metal charge transfer transitions in various minerals. Canadian Mineralogist, 15, 500–507.

Smith, G. and Strens, R.G.J. (1976) Intervalence transfer absorption in some silicate, oxide and phosphate minerals. In: The Physics and Chemistry of Minerals and Rocks (Strens, R.G.J. ed.), Wiley, New York, 583–612.

Taran, M.N. and Langer, K. (1998) Temperature and pressure dependencies of intervalence charge transfer bands in spectra of Fe- and Fe,Ti-bearing oxygen-based minerals. Neues Jahrbuch für Mineralogie. Abhandlungen, 172, 325–346.

——— (2000) Electronic absorption spectra of Fe^{3+} in andradite and epidote at different temperatures and pressures. European Journal of Mineralogy, 12, 7–15.

——— (2001) Electronic absorption spectra of Fe^{2+} ions in oxygen-based rock-forming minerals at temperatures between 297 and 600 K. Physics and Chemistry of Minerals, 28, 199–210.

Taran, M.N. and Rossman, G.R. (2001) Optical spectroscopic study of tuhualite and a re-examination of the beryl, cordierite and osumilite spectra. American Mineralogist, 86, 973–980.

Taran, M.N., Platonov, A.N., and Polshyn, E.V. (1978) Color of gem garnets from USSR deposits. Konstitutsiya i svoistva mineralov, N12, 88–103 (in Russian)

Volkov, S. Yu., Grechushnikov, B.N., Sevastyanov, B.K., and Tsvetkov, V.B. (1981) A sapphire cold finger for getting intermediate temperatures. Pribory i technika experimenta, 2, 251–253 (in Russian).

Whipple, E.R. (1973) Quantitative Mössbauer spectra and chemistry of iron. Ph.D. thesis, M.I.T., 187 pp.

White, W.B. and Moore, R.K. (1972) Interpretation of the spin allowed bands of Fe^{2+} in silicate garnets. American Mineralogist, 57, 1692–1710.

Manuscript received November 22, 2005
Manuscript accepted November 30, 2006
Manuscript handled by Robert Dymek